## CONDENSED MATTER

# Optical Levitation of Mie-Resonant Silicon Particles in the Field of Bloch Surface Electromagnetic Waves

## D. A. Shilkin[a], * and A. A. Fedyanin[a]

*[a] Faculty of Physics, Moscow State University, Moscow, 119991 Russia*
***e-mail: shilkin@nanolab.phys.msu.ru**

Manipulating the motion of nanoparticles in liquid media using the near field of integrated optical elements is associated with enhanced viscous friction and an increased probability of adhesion. One of the ways to overcome these difficulties is the search for systems with a minimum of potential energy located at a distance from the structure surface. In this paper, we numerically study the forces acting on Mie-resonant silicon particles in water in the evanescent field of a Bloch surface wave and propose a method for localizing such particles at a controlled distance from the surface. For this purpose, we use surface waves at two optical frequencies, which provide different signs of interaction with the particle and different depths of field penetration into the medium. As an example, we consider a silicon sphere with a diameter of 130 nm in the field of laser radiation with wavelengths of 532 and 638 nm and a total power of 100 mW; taking into account the Brownian motion, we show that the proposed method provides stable particle localization at an equilibrium distance to the surface, adjustable in the range from 60 to 100 nm.

Modern optical manipulation techniques that employ integrated optical elements make it possible to localize, move, and sort micro- and nanoparticles in compact microfluidic devices [1, 2]. Channel and slot optical waveguides [3–5], photonic crystal structures [6, 7], and ring microcavities [8, 9] can be used for these purposes. A few years ago, it was proposed to employ one-dimensional photonic crystals supporting Bloch surface waves as a novel platform for integrated optics [10–13]. These waves are characterized by low losses in a wide range of wavelengths, and their dispersion properties can be controlled by varying the structure geometry [14]. Bloch surface waves have shown their effectiveness in the optical manipulation of micro- and nanoparticles. It has been experimentally demonstrated that they can be used to move polystyrene microspheres [15], trap metal nanoparticles [16], and assemble biological cells near the photonic crystal surface [17].

Due to the increased interest in optical resonances of high-index non-metallic particles, suspensions of submicron silicon particles have been actively studied in recent years [18–20]. It has been shown that the resonant dependence of the light pressure force on the particle size, which is characteristic of such suspensions [21, 22], makes it possible to use them for selective laser printing of Mie-resonant structures [23], while enhanced optical binding effects in pairs of silicon spheres can be exploited for the development of dynamically tunable nanoantennas [24]. It has been

experimentally demonstrated that conventional optical tweezers based on a tightly focused Gaussian beam can be used for the optical trapping of such particles [25]. At the same time, the possibilities of manipulating Mie-resonant silicon particles by using the near field of micro- and nanostructures remain largely unexplored.

In integrated optical manipulation schemes, particles are typically attracted to the structure by optical gradient forces, while electrostatic repulsion forces keep them at a distance from the surface and prevent adhesion [26]. The need to provide electrostatic repulsion limits the choice of suspensions that can be studied and forces the use of surfactants [5, 6]. In this case, the position of the particles in the direction perpendicular to the surface remains uncontrolled. For some systems, for example, for Mie-resonant particles near a metal surface, a stable equilibrium position was theoretically predicted to exist at a finite distance from the surface due to the hybridization of scattering resonances near the surface [27–29]. The ability to manipulate particles, keeping them at a distance by optical methods, is attractive because it allows minimizing viscous friction and adhesion probability. The use of metals, however, is often accompanied by their heating and the emergence of convection currents, which significantly affect the movement of particles [30].

For the optical trapping of atoms in the near field of waveguide structures, the problem of forming a potential energy minimum at a distance from the sur-
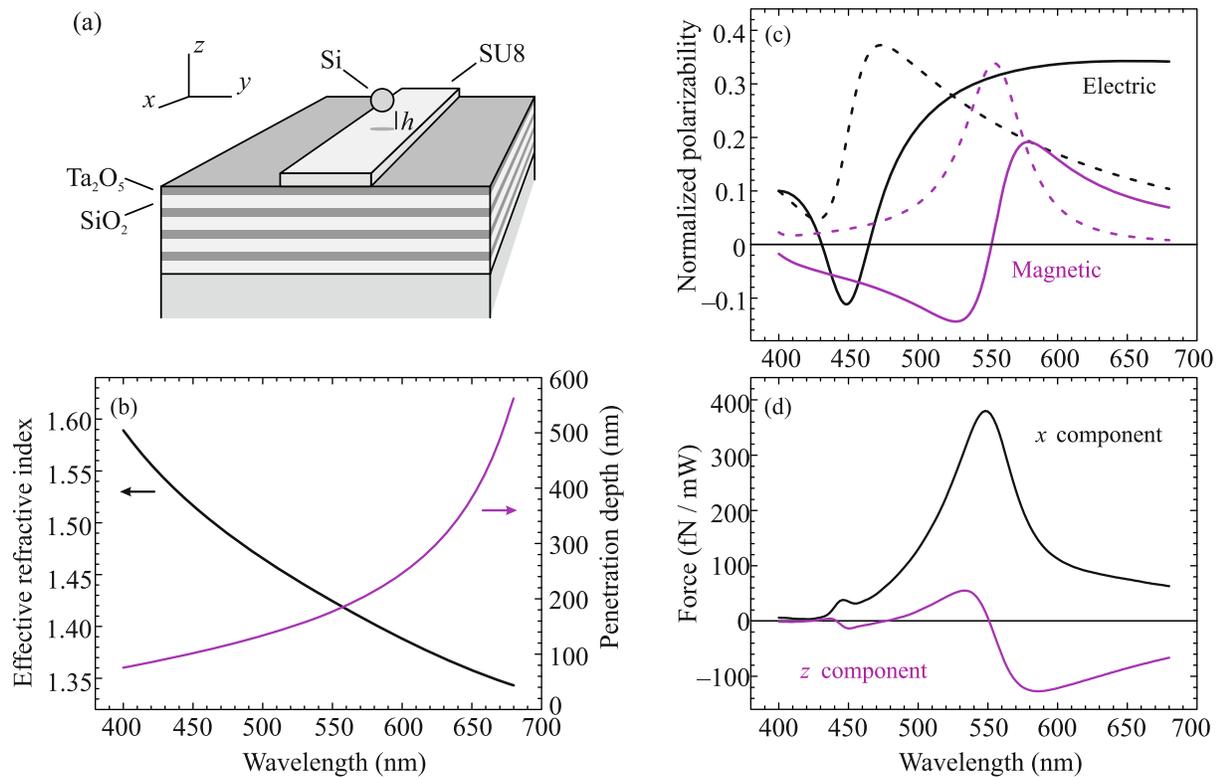
**Fig. 1.** (Color online) (a) Schematic of the structure. The surface wave excitation region is confined to a waveguide directed along the $x$-axis; the particle is localized in water, forming a gap $h$ with the surface of the waveguide. (b) Effective refractive index and penetration depth of the Bloch surface wave as a function of the wavelength. (c) Electric and magnetic polarizabilities of a spherical silicon particle with a diameter of 130 nm, normalized to the particle volume. Solid lines show the real parts and the dashed ones show the imaginary parts. (d) Normal and tangential components of the optical force acting on a 130-nm silicon particle at $h = 30$ nm versus the wavelength of light; the force values are normalized to the optical power in the surface wave mode.

face has been solved both theoretically [31, 32] and experimentally [33], using light of two wavelengths. Since the polarizability of atoms near the transition frequency changes sign, the forces acting in optical fields with wavelengths oppositely detuned from the transition frequency have opposite directions. If, in this case, the degree of field localization depends on the wavelength, for a certain range of power ratios, these forces balance each other at a finite distance from the structure. Such an approach can be useful not only for trapping atoms but also for manipulating high-refractive-index micro- and nanoparticles, whose polarizability changes sign near Mie scattering resonances; however, to the best of our knowledge, its applicability to this case has not been previously explored.

In this work, we numerically study the forces acting on Mie-resonant silicon particles in the evanescent field of a Bloch surface wave propagating in an all-dielectric structure and propose a method for particle localization at a controlled distance from the surface using surface waves at two optical frequencies.

The scheme of the structure under study is shown in Fig. 1a. The photonic crystal consists of four pairs of silicon dioxide and tantalum pentoxide layers on a glass substrate. The layer thicknesses are 220 and 155 nm, respectively, which provides a photonic band-gap with a central wavelength of 1.3 $\mu$m at normal incidence [34]. The Bloch surface wave propagation region is confined to a polymer strip 1 $\mu$m wide and 200 nm high, which acts as a channel waveguide. The strip material is SU8 photopolymer, which has been previously successfully used to fabricate similar structures [13, 35]. A spherical silicon particle is localized in water, forming a gap $h$ with the waveguide surface.

Numerical calculations were carried out by the finite-difference time-domain method using *Lumerical FDTD Solutions* software. In the calculations, we used dispersion data for water [36], crystalline silicon [37], silicon oxide and tantalum oxide films [38], and data from manufacturers of SU8 photopolymer and Schott D263T glass. The simulation region was a cube with an edge length of 6 $\mu$m and a nonuniform grid. On all faces of the cube, absorbing boundary conditions in the form of perfectly matched layers were set, and the antisymmetry condition was set on the vertical plane passing through the axis of the waveguide. A source generating a femtosecond pulse with a broad

spectrum in the Bloch surface wave mode was used in the model. After simulating the pulse propagation in the studied system, the field at the frequencies of interest was calculated by the Fourier transform. The force values were determined by integrating the components of the Maxwell stress tensor in the Minkowski form over the surface of a cube containing the particle and normalized to the energy of light propagating in the Bloch surface wave mode. To verify the obtained results, we carried out additional calculations with an increase in the grid density and the simulation region size at a minimum gap between the particle and the waveguide surface $h = 15$ nm; the differences in the results were no more than 2%.

In the area covered by the polymer film, the studied photonic crystal supports the propagation of $s$-polarized Bloch surface waves. The spectral properties of the fundamental mode of the structure under study are shown in Fig. 1b. Here, the penetration depth of the surface wave field $d_{pen}$ is defined as the distance from the structure surface at which the electric field amplitude decreases by a factor of $e$. It is related to the effective refractive index of the mode $n_{eff}$ as follows:

$$\frac{1}{d_{pen}} = \frac{2\pi}{\lambda}\sqrt{n_{eff}^2 - n_e^2},\qquad(1)$$

where $n_e$ is the environment refractive index, and $\lambda$ is the light wavelength in vacuum. As the wavelength increases, the effective refractive index of the mode decreases, and the depth of the field penetration into water increases. For example, for typical wavelengths of available laser sources of 532 and 638 nm, the penetration depth is 159 and 339 nm, respectively. If the light of two optical frequencies simultaneously propagates in the structure, the relative contribution of the low-frequency component increases with distance from the surface.

Optical forces acting on subwavelength silicon particles in the visible range are primarily determined by the electric and magnetic dipole polarizabilities [39, 40]. Figure 1c shows the spectral dependences of these quantities, calculated in accordance with the Mie theory [39] and plotted for a silicon sphere with a diameter of 130 nm. One of the properties of forced oscillations is the phase change by $\pi$ as the frequency of the driving force passes through the resonant frequency of the system. Thus, near the magnetic dipole and electric dipole resonances of the sphere, the real part of the corresponding polarizability changes sign. In an inhomogeneous electromagnetic field, this leads to a change in the direction of the optical gradient force.

The calculated force acting on a silicon particle with a diameter of 130 nm is shown in Fig. 1d. Here, the gap between the waveguide surface and the particle was set to $h = 30$ nm; the calculated values were normalized to the optical power in the fundamental surface wave mode. In the vicinity of the magnetic dipole
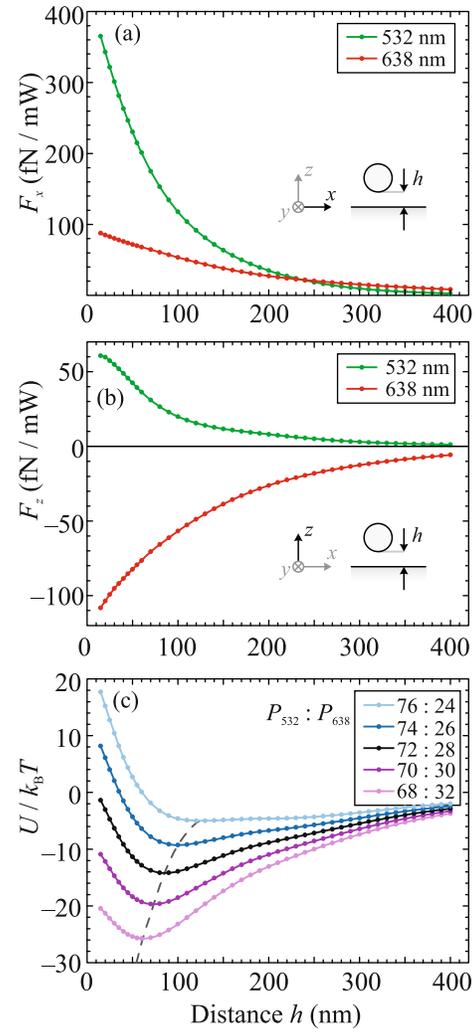


**Fig. 2.** (Color online) (a) Tangential and (b) normal components of the optical force acting on a 130 nm silicon particle in the Bloch surface wave field versus the gap between the waveguide surface and the particle $h$; the force values are shown for vacuum wavelengths of 532 and 638 nm and normalized to the optical power in the surface wave mode. (c) Potential energy of a 130 nm particle in the field of Bloch surface waves of two colors with a total power of 100 mW and different power ratios. The gray dashed line shows the trajectory of the displacement of the stable equilibrium position.

resonance, the tangential component of the force reaches its maximum value due to the high scattering efficiency. At the same time, the normal component changes sign. If the light wavelength is more than 551 nm, the particle is attracted to the surface, and if it lies in the range from 477 to 551 nm, the particle is repelled from the surface.

Let us now consider the forces acting in the studied system when two laser sources with wavelengths of 532 and 638 nm are used. Figures 2a and 2b show the dependences of the tangential and normal components of the optical force on the gap between the wave-
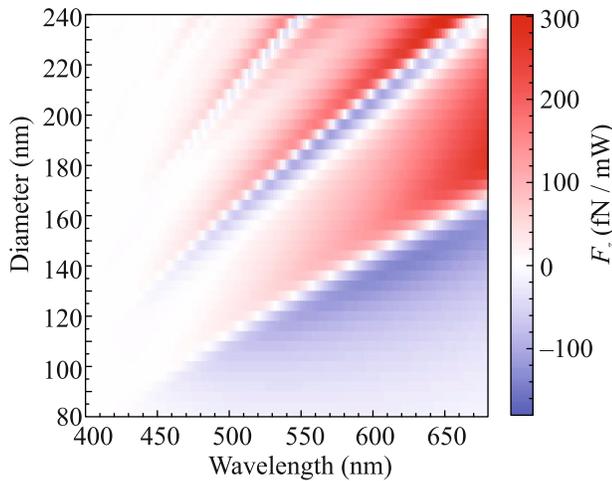
**Fig. 3.** (Color online) Dependence of the normal component of the force acting on a silicon particle in the field of a Bloch surface wave on the light wavelength and particle diameter. The gap between the waveguide surface and the particle is fixed and equal to $h = 30$ nm; the force values are normalized to the optical power in the surface wave mode.

guide surface and the particle $h$, calculated for a 130-nm silicon sphere in the field of surface waves at the selected wavelengths. With increasing distance from the surface, both components tend to zero, and this happens faster in the case of green light. The tangential component for both wavelengths acts in the surface wave propagation direction. The normal component attracts particles to the waveguide in the case of red light and repels in the case of green light.

With the simultaneous use of light at two frequencies, the optical forces are summed up, and in the direction perpendicular to the surface, a stable equilibrium position can be formed at a finite distance from the surface. Figure 2c shows the potential energy profile along the axis perpendicular to the surface obtained by integrating the normal component of the optical force. The potential energy values are normalized to $k_BT$, where $k_B$ is the Boltzmann constant, and $T = 298$ K is the room temperature. The total optical power is fixed and is $P_{532} + P_{638} = 100$ mW, while the power ratio $P_{532} : P_{638}$ is varied. Along with this, the shape of the potential changes and the stable equilibrium position shifts. At a power ratio of 70 : 30, the minimum potential energy corresponds to the size of the gap between the waveguide surface and the particle $h = 73$ nm, and at a ratio of 74 : 26, it corresponds to the gap size $h = 100$ nm. Note that along with the shift of the energy minimum, the stiffness and the depth of the potential well change. In optical manipulation, a standard criterion for stable trapping is the potential depth of the order of $10k_BT$ or more [2]. In the given example, this condition is satisfied for those profiles

that have the minimum at the gap $h$ from 60 to 100 nm. The use of higher powers will further expand this range.

The results presented above have been obtained for a fixed particle diameter. As the particle size increases, Mie resonances shift towards longer wavelengths [22, 41]. Figure 3 shows the normal component of the optical force as a function of the particle diameter and vacuum wavelength for a fixed gap between the waveguide surface and the particle $h = 30$ nm. As the size increases, the spectral regions of repulsion shift towards longer wavelengths, and in the visible range, resonances of higher orders begin to manifest themselves. Finally, we note that the spectral properties of one-dimensional photonic crystals are determined by the thicknesses of their layers [42], which makes it possible to optimize the structure for manipulating particles of various sizes using available laser sources. A similar approach can find applications in other systems, including Mie-resonant particles in the field of conventional channel waveguides and optical fibers.

In conclusion, the optical forces acting on submicron silicon particles in the Bloch surface wave field can attract particles to the structure surface and repel them from it, depending on the light wavelength and particle size. Using light of two optical frequencies, one can achieve particle localization at a finite distance from the surface, the value of which is determined by the ratio of the powers at the frequencies used. The proposed method makes it possible to minimize friction when moving particles along the surface and eliminate the possibility of adhesion to the structure.

## CONFLICT OF INTEREST

The authors declare that they have no conflicts of interest.

## REFERENCES

1. D. Erickson, X. Serey, Y.-F. Chen, and S. Mandal, LabChip **11**, 995 (2011).

2. M. Daly, M. Sergides, and S. N. Chormaic, Laser Photon. Rev. **9**, 309 (2015).

3. K. Grujic, O. G. Helleso, J. P. Hole, and J. S. Wilkinson, Opt. Express **13**, 1 (2005).

4. B. S. Schmidt, A. H. J. Yang, D. Erickson, and M. Lipson, Opt. Express **15**, 14322 (2007).

5. A. H. J. Yang, S. D. Moore, B. S. Schmidt, M. Klug, M. Lipson, and D. Erickson, Nature (London, U.K.) **457**, 71 (2009).

6. S. Mandal, X. Serey, and D. Erickson, Nano Lett. **10**, 99 (2010).

7. M. G. Scullion, Y. Arita, T. F. Krauss, and K. Dholakia, Optica **2**, 816 (2015).

8. S. Lin, E. Schonbrun, and K. Crozier, Nano Lett. **10**, 2408 (2010).

9. H. Cai and A. W. Poon, Opt. Lett. **35**, 2855 (2010).

10. L. Yu, E. Barakat, T. Sfez, L. Hvozdara, J. di Francesco, and H. P. Herzig, Light Sci. Appl. **3**, e124 (2014).

11. E. A. Bezus, L. L. Doskolovich, D. A. Bykov, and V. A. Soifer, JETP Lett. **99**, 63 (2014).

12. T. Kovalevich, D. Belharet, L. Robert, G. Ulliac, M.-S.Kim, H. P. Herzig, T. Grosjean, and M.-P. Bernal, Appl. Opt. **58**, 1757 (2019).

13. K. R. Safronov, D. N. Gulkin, I. M. Antropov, K. A. Abrashitova, V. O. Bessonov, and A. A. Fedyanin, ACS Nano **14**, 10428 (2020).

14. W. M. Robertson, J. Lightwave Technol. **17**, 2013 (1999).

15. D. A. Shilkin, E. V. Lyubin, I. V. Soboleva, and A. A. Fedyanin, Opt. Lett. **40**, 4883 (2015).

16. Y. Xiang, X. Tang, Y. Fu, F. Lu, Y. Kuai, C. Min, J. Chen, P. Wang, J. R. Lakowicz, X. Yuan, and D. Zhang, Nanoscale **12**, 1688 (2020).

17. F. Lu, L. Gong, Y. Kuai, X. Tang, Y. Xiang, P. Wang, and D. Zhang, Photon. Res. **10**, 14 (2022).

18. L. Shi, J. T. Harris, R. Fenollosa, I. Rodriguez, X. Lu, B. A. Korgel, and F. Meseguer, Nat. Commun. **4**, 1904 (2013).

19. W. Chaâbani, J. Proust, A. Movsesyan, J. Béal, A.-L. Baudrion, P.-M. Adam, A. Chehaidar, and J. Plain, ACS Nano **13**, 4199 (2019).

20. V. Valuckas, R. Paniagua-Domínguez, A. Maimaiti, P. P. Patra, S. K. Wong, R. Verre, M. Käll, and A. I. Kuznetsov, ACS Photon. **6**, 2141 (2019).

21. A. V. Maslov and V. N. Astratov, Appl. Phys. Lett. **105**, 121113 (2014).

22. D. A. Shilkin, E. V. Lyubin, M. R. Shcherbakov, M. Lapine, and A. A. Fedyanin, ACS Photon. **4**, 2312 (2017).

23. C. Zaza, I. L. Violi, J. Gargiulo, G. Chiarelli, L. Schumacher, J. Jakobi, J. Olmos-Trigo, E. Cortes, M. König, S. Barcikowski, S. Schlücker, J. J. Sáenz, S. A. Maier, and F. D. Stefani, ACS Photon. **6**, 815 (2019).

24. T. Yano, Y. Tsuchimoto, R. P. Zaccaria, A. Toma, A. Portela, and M. Hara, Opt. Express **25**, 431 (2017).

25. A. Andres-Arroyo, B. Gupta, F. Wang, J. J. Gooding, and P. J. Reece, Nano Lett. **16**, 1903 (2016).

26. P. Schein, P. Kang, D. O'Dell, and D. Erickson, Nano Lett. **15**, 1414 (2015).

27. A. V. Maslov, Opt. Lett. **42**, 3327 (2017).

28. A. V. Maslov, Ann. Phys. **532**, 2000129 (2020).

29. E. Bulgakov, K. Pichugin, and A. Sadreev, Phys. Rev. A **103**, L051501 (2021).

30. J. Chen, J.F.-C. Loo, D. Wang, Y. Zhang, S.-K. Kong, and H.-P. Ho, Adv. Opt. Mater. **8**, 1900829 (2020).

31. A. H. Barnett, S. P. Smith, M. Olshanii, K. S. Johnson, A. W. Adams, and M. Prentiss, Phys. Rev. A **61**, 023608 (2000).

32. F. le Kien, V. I. Balykin, and K. Hakuta, Phys. Rev. A **70**, 063403 (2004).

33. E. Vetsch, D. Reitz, G. Sagué, R. Schmidt, S. T. Dawkins, and A. Rauschenbeutel, Phys. Rev. Lett. **104**, 203603 (2010).

34. A. Yariv and P. Yeh, *Optical Waves in Crystals* (Wiley, New York, 1984).

35. K. A. Abrashitova, D. N. Gulkin, K. R. Safronov, N. G. Kokareva, I. M. Antropov, V. O. Bessonov, and A. A. Fedyanin, Appl. Sci. **8**, 63 (2018).

36. D. J. Segelstein, Master Thesis (Univ. Missouri, Kansas City, 1981).

37. M. A. Green, Sol. Energy Mater. Sol. Cells **92**, 1305 (2008).

38. L. V. Rodríguez-de Marcos, J. I. Larruquert, J. A. Méndez, and J. A. Aznárez, Opt. Mater. Express **6**, 3622 (2016).

39. M. Nieto-Vesperinas, R. Gomez-Medina, and J. J. Saenz, J. Opt. Soc. Am. A **28**, 54 (2011).

40. L. Shi and F. Meseguer, Opt. Express **20**, 22616 (2012).

41. A. B. Evlyukhin, C. Reinhardt, A. Seidel, B. S. Luk'yanchuk, and B. N. Chichkov, Phys. Rev. B **82**, 045404 (2010).

42. K. R. Safronov, V. O. Bessonov, and A. A. Fedyanin, JETP Lett. **114**, 321 (2021).

*Translated by the authors*